Searching for numerically simulated signals from black-hole binaries with a phenomenological template family

2009 Class. Quantum Grav. 26 114010

(http://iopscience.iop.org/0264-9381/26/11/114010)

IOP PUBLISHING CLASSICAL AND QUANTUM GRAVITY

Class. Quantum Grav. **26** (2009) 114010 (13pp) doi:10.1088/0264-9381/26/11/114010

Searching for numerically simulated signals from black-hole binaries with a phenomenological template family

Lucía Santamaría[1], Badri Krishnan[1] and John T Whelan[1,2]

[1] Max-Planck-Institut für Gravitationsphysik (Albert-Einstein-Institut), Am Mühlenberg 1, D-14476 Potsdam, Germany
[2] Center for Computational Relativity and Gravitation and School of Mathematical Sciences, Rochester Institute of Technology, 85 Lomb Memorial Drive, Rochester, NY 14623, USA

E-mail: lucia.santamaria@aei.mpg.de

Received 8 January 2009, in final form 3 March 2009
Published 19 May 2009
Online at stacks.iop.org/CQG/26/114010

Abstract
Recent progress in numerical relativity now allows computation of the binary black-hole merger, whereas post-Newtonian and perturbative techniques can be used to model the inspiral and ringdown phases. So far, most gravitational-wave searches have made use of various post-Newtonian-inspired templates to search for signals arising from the coalescence of compact binary objects. Ajith *et al* have produced hybrid waveforms for non-spinning binary black-hole systems which include the three stages of the coalescence process, and constructed from them phenomenological templates which capture the features of these waveforms in a parametrized form. As a first step towards extending the present inspiral searches to higher-mass binary black-hole systems, we have used these phenomenological waveforms in a search for numerically simulated signals injected into synthetic LIGO data as part of the NINJA project.

PACS numbers: 04.80.Nn, 04.30.Db, 04.25.Nx, 04.25.dc

(Some figures in this article are in colour only in the electronic version)

1. Introduction

An international network of ground-based gravitational-wave (GW) detectors (LIGO [1], Virgo [2], GEO600 [3]) operating roughly in the 10^1 to 10^4 Hz band has recently finished taking data at or close to design sensitivity, and the worldwide LIGO Scientific Collaboration (LSC) and Virgo Collaboration are currently involved in analysing it. Furthermore, space-based instruments, such as the Laser Interferometer Space Antenna (LISA) [4, 5], are also expected to probe a significantly lower-frequency stretch of the GW spectrum, namely the

10^{-4} to 10^{-1} Hz band. One of the most promising candidate sources for detection is a compact binary system, composed of either neutron stars or black holes. GW emission from such systems, in particular from those consisting of binary black holes (BBHs), is expected to be detected by these instruments in the near future, giving rise to the new field of gravitational-wave astronomy.

The detection of gravitational signals arising from the coalescence of a BBH system, as well as the estimation of its physical parameters, relies heavily on the ability to accurately model the waveforms emitted during the inspiral, merger and ringdown stages of the process. Until recently, the usual approach to the problem consisted entirely of making use of analytical approximations to the full theory of general relativity. Thus, a post-Newtonian (PN) expansion would be used to solve Einstein equations in the initial inspiral part of the coalescence (see [6] and references therein), while perturbation theory would be applied to the final ringdown after the two black holes have merged together. The intermediate phase corresponding to the strongest gravitational signal remained unmodelled until the breakthroughs occurred in 2005 [7–9], when several numerical-relativity (NR) groups finally succeeded in using their numerical codes to solve for the merger and ringdown phases of the BBH coalescence, calculating the gravitational waves associated with the process. Steady progress quickly followed those pioneering results, leading to a thriving era in the field.

Among the most suitable data-analysis (DA) methods currently used to look for signals from compact binary coalescences in the output data of GW interferometers is the matched-filter search technique against a given class of template waveforms. So far, most current LSC searches for compact binaries in the LIGO/Virgo data have made use of different flavours of analytical PN templates to search for gravitational waves [10, 11]. Further efforts have been undertaken in the recent past to incorporate the full inspiral-merger-ringdown (IMR) waveforms with information from NR results in the different DA packages into the LSC Algorithm Library [12]. These include the EOBNR waveforms based on the effective-one-body approach [13] and the phenomenological waveforms resulting from hybrid PN-NR match [14–16] among others.

In order to be able to make confident statements about the performance of diverse DA pipelines and their ability to find true gravitational waves, data analysts have developed several techniques, one of which consists of studying the pipeline's response to signals introduced in the detector strain as *software injections*. This procedure helps understand the background noise present in the detector data and provides insight for fine-tuning the numerous parameters and thresholds in the different analyses. Since the strongest burst of gravitational radiation originates during the BBH merger, a good test to check the effectiveness of existing DA techniques is to inject NR signals that contain the final part of the coalescence into simulated LIGO/Virgo data and proceed with the GW searches.

An open collaboration under the acronym NINJA [17] has been created that aims at fostering closer interaction between numerical relativists and data analysts. Its immediate purpose is to understand the sensitivity of current DA pipelines to binary black-hole NR signals buried in simulated noise. To that effect, a set of waveforms was injected into LIGO- and Virgo-like noise, within the mass and distance ranges displayed in figure 1. For the numerical waveforms that were used see [7, 8, 18–31], for descriptions of the numerical codes see [23, 28, 31–40]. Several data analysis groups took part in the NINJA project, employing their data-analysis codes to search for the NR signals. A comprehensive compilation of the goals and results arising from the NINJA Collaboration can be found in a dedicated paper [41].

This paper presents the results of a search for BBH signals in the NINJA data, employing a new template bank based on a phenomenological model for non-spinning BBH systems by Ajith *et al* [14–16]. These waveforms fully describe the three stages of the coalescence of two non-spinning black holes for small mass ratios and, if implemented in current GW searches, should represent a step forward with respect to PN templates that do not account for the merger and ringdown phases of the process. The remainder of the paper is organized as follows. In section 2, we introduce the data-analysis pipeline developed by the compact binary coalescence (CBC) group of the LSC to search for signals from compact binaries in the LIGO/Virgo data. In section 3, we describe the modifications performed in the pipeline that allow the use of the phenomenological waveforms as a new search template. In section 4, we present the results obtained when applying this new template family to a search in the NINJA data. Finally, in section 5, we review our main conclusions and propose future improvements and directions for further research.

2. The inspiral pipeline

The LSC inspiral pipeline infrastructure developed by the CBC group has been employed to analyse the data released for the NINJA project. The pipeline, without major conceptual modifications, has been used in LSC searches for compact binaries from the third LIGO science run onwards [10, 11]. The same pipeline has been modified for the analysis of the NINJA data with the phenomenological template family described in section 3. Since the signals present in the simulated noise are known to be NR simulations of BBH coalescences, the search method consists of a matched-filter technique [42] using an IMR waveform model based on the hybrid NR-PN waveforms as described below. The findings presented here concentrate solely on the simulated LIGO detectors H1, H2 and L1, although the NINJA data were generated for the simulated Virgo interferometer V1 as well.

The LSC inspiral pipeline performs a series of hierarchical operations in order to search for real signals buried in the detector noise. The first stage is the construction of a suitable template bank covering the desired parameter space, and for which the overlap between any point and the nearest is at least as large as a certain minimal match [43–45], assuming the following definition of inner product in the space of template waveforms

$$\langle a|b\rangle \equiv 4\,\mathrm{Re}\left[\int_{f_{\min}}^{f_{\max}} \frac{\tilde{a}(f)\tilde{b}^{\star}(f)}{S_h(f)}\,\mathrm{d}f\right]. \tag{1}$$

Here $S_h(f)$ represents the one-sided noise spectral density of the detector and the tilde denotes the Fourier transform operation. The overlap between templates can be quantified by computing the inner product of the normalized waveforms and maximizing it over their extrinsic parameters (time and phase shifts). In the analysis here presented we set the value of the minimal match

$$\mathcal{M} = \max_{\tau,\Phi} \frac{\langle a|b\rangle}{\sqrt{\langle a|a\rangle\langle b|b\rangle}} \tag{2}$$

between elements of our phenomenological template to 0.99, which ensures an event loss of less than 3% due to mismatch between real signals and templates. After a filtering process through the desired template bank, the triggers that pass a certain signal-to-noise (SNR) ratio threshold are checked for coincidence in time and masses between two or three detectors. For our analyses, an SNR threshold of 5.5 was employed, in agreement with the value currently used in recent LSC searches for binary coalescences [11]. Whenever triggers are found with comparable coalescence time and parameters (in this case, component masses), they are stored as coincident [46]. The detection statistic is the combined SNR of the single detector triggers.

Once the initial matched filter has produced a list of triggers that pass the first coincidence step, a second stage follows where data are again filtered, but only through the templates that previously matched a trigger. Additionally the χ^2 [47] and r^2 [48] signal-based vetoes, designed to separate true inspiral signals from fluctuations in non-stationary noise, are applied. At this point an effective SNR $\rho_{\mathrm{eff},i}\left(\rho_i, \chi_i^2\right)$ is calculated combining the standard SNR with the χ^2 value characterizing the mismatch between the spectral content of the template and the data. After further coincidence tests, the surviving triggers are listed as true gravitational wave candidates and constitute the output of the search. The significance of the triggers is based on the combined effective SNR, namely

$$\rho_{\mathrm{eff}} = \sqrt{\sum_i^N (\rho_{\mathrm{eff},i})^2}. \tag{3}$$

A direct comparison between the list of injections performed on the NINJA noise and the triggers found by the pipeline allows for conclusions about the sensitivity of the analysis and the relative performance of the different template banks.

3. The phenomenological template bank

Most standard searches for gravitational waves from BBHs use the PN approximation of general relativity to construct banks of templates that account for the inspiral stage of the coalescence process, and the final ringdown can also be computed via perturbative techniques. However, the full calculation of the waveform in the merger stage requires numerical methods. These numerical simulations are in general rather expensive, and it is at present not feasible to model a coalescing binary over hundreds of orbits with sufficient accuracy. It is in fact also unnecessary to do so, because PN theory provides a valid description of the system when the black holes are sufficiently separated and the gravitational field is weak. Thus, a promising approach for constructing long waveform models covering the inspiral, merger and ringdown regimes is to stitch together the results of PN and NR calculations.

One procedure for constructing such hybrid waveforms is presented in [14–16], where PN and NR waveforms are matched in an appropriate regime ($-750 \leqslant t/M \leqslant -550$) prior to the merger ($M$ is the total mass of the binary system in solar masses). Restricted 3.5PN waveforms at mass-quadrupole order are used for the inspiral phase, as given by equation (3.1) of [15]. For the numerical part, the model is based on long unequal-mass waveforms from simulations run by the Jena group using the `BAM` code [32, 49, 50]. These simulations span a range of mass ratios corresponding to $0.16 \leqslant \eta \leqslant 0.25$, where $\eta = (m_1 m_2)/M^2$ is the so-called symmetric mass ratio of the binary system. The matching of PN and NR data is performed over an overlapping region, under the assumption that both approaches to the true BBH waveform are approximately correct at the late inspiral stage. Once the hybrid waveforms are constructed, they are fit to a phenomenological model determined entirely by the physical parameters of the binary system. This fit to an analytical expression is performed in the Fourier domain, assuming a functional dependence of the form

$$u(f) = A_{\mathrm{eff}}(f)\, \mathrm{e}^{\mathrm{i}\Psi_{\mathrm{eff}}(f)}, \tag{4}$$

with amplitude and phase given by equations (11) and (14) of [15]. Each waveform is parametrized by the physical parameters of the system, which in the non-spinning case are solely the masses m_1 and m_2 of the black holes. As a result of the matching and fitting procedures described above, a two-dimensional template family of waveforms that attempt to model the entire coalescence of non-spinning binary black-hole systems has been obtained.

The phenomenological template bank has been included in the LSC inspiral pipeline routinely used by the CBC group as a new waveform for filtering in the time domain. A search

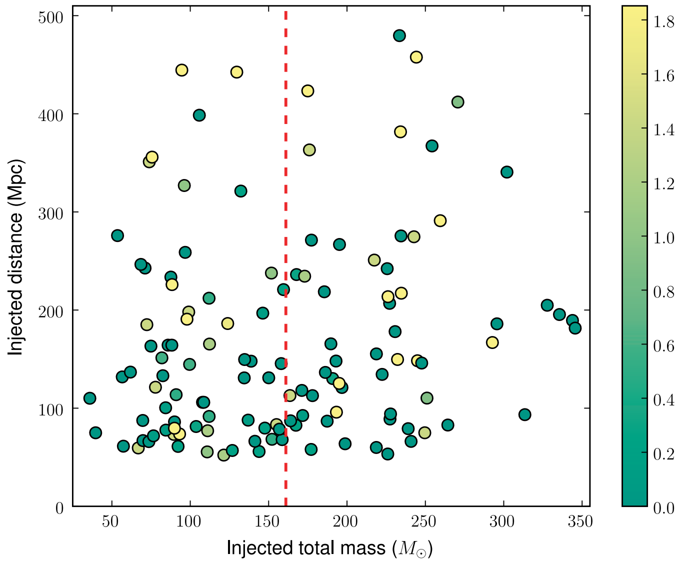

Figure 1. Total mass and distance of the NINJA injected signals, with the colour code encoding the modulus of the dimensionless total spin $|\vec{S}_1/m_1^2 + \vec{S}_2/m_2^2|$ of the black holes. The total mass of the injected signals lies within the range $36\,M_\odot \leqslant M \leqslant 460\,M_\odot$ and they are located at a distance between 52 and 480 Mpc. The vertical line delimits the mass parameter space with $M < 160\,M_\odot$ that our phenomenological template bank covers. The full NINJA data set spans a duration of a little over 30 h and contains a total of 126 signals injected in simulated noise, 67 of which overlap with the parameter space of our template bank.

on the NINJA data has been performed, within a mass range of $20\,M_\odot \leqslant m_1, m_2 \leqslant 80\,M_\odot$ for the component masses, with $40\,M_\odot \leqslant M \leqslant 160\,M_\odot$ for the total mass of the binary. A technical issue regarding construction of high mass waveforms prevented us from using a parameter space that completely overlaps with the mass range of the injected NINJA signals (see figure 1), which might negatively affect the capability for recovering high-mass signals. Further searches for prospective NINJA projects will greatly benefit from inclusion of high-mass templates, and a fix for this issue is underway. The template bank is constructed using the standard second-order post-Newtonian metric, and uses a hexagonal placement algorithm in mass space with a minimal match of 0.99 [45]. Note that we have not implemented the new metric correspondent to the phenomenological waveforms, which might be significantly different than the standard 2PN metric; however, as we shall see, the current template bank placement suffices for detection purposes and for moderately accurate parameter estimation. The number of signals that are recovered by the pipeline depends strongly on the choice for the upper frequency cutoff used in the matched filter integral, as we have observed in our investigations with the integration stopping at the ISCO (innermost stable circular orbit, $r = 6M$), light ring (the unstable circular orbit for photons orbiting a Schwarzschild black hole, $r = 3M$) and Lorentzian ringdown (LRD)[3] frequencies.

In figure 2, we show two waveforms from our phenomenological template bank, which correspond to equal-mass binaries in the corners of our parameter space, namely total mass $M = 40\,M_\odot$ and $160\,M_\odot$. Displayed are both the original time domain waveform and its 'whitened' form [51], as the initial LIGO detector perceives it, and the relative amplitudes

[3] This is 1.2 times the fundamental ringdown frequency of [54].

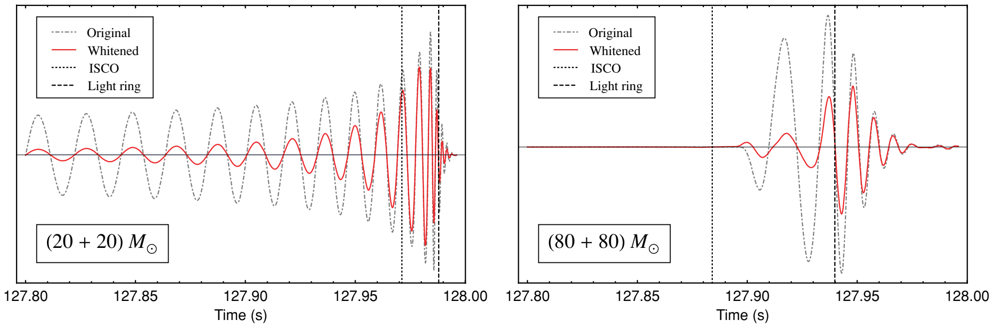

Figure 2. The figure shows two time-domain phenomenological waveforms from the template bank used in this search, corresponding to equal-mass binaries in the corners of our parameter space, namely $(20 + 20)M_\odot$ and $(80 + 80)M_\odot$ BBH systems. The original and 'whitened' [51] waveforms are shown, with their amplitudes arbitrarily resized. The dotted and dashed vertical lines mark the points where the ISCO and light ring frequencies are reached. The LRD frequency is not shown, since it basically extends up to the full waveform. A matched-filter search that starts at 30 Hz and ends at the ISCO will not be able to pick the most massive binaries, since the inspiral phase of the coalescence falls below the LIGO interferometers' detection band. It is expected that the light ring and LRD frequencies, which extend up to the BH merger and ringdown respectively, will show improved performance at recovering high-mass signals.

have been arbitrarily resized. The whitened waveform is computed as the inverse Fourier transform of the original signal multiplied by the function $1/\sqrt{S_h(f)}$ in the frequency domain, where $S_h(f)$ is the one-sided noise power spectral density of the simulated LIGO detectors. In each plot the vertical lines correspond to the ISCO and light ring frequencies. In our searches we have started filtering against the phenomenological templates at either 30 or 40 Hz and we have stopped the integration at the three frequencies discussed in the above paragraph. It is evident that whereas a cut at the ISCO frequency still retains a good portion of the inspiral signal for low-mass binaries, it is insufficient for higher masses. The light ring and LRD frequencies, on the other hand, extend roughly up to the BH merger and to the Lorentzian tail (from the decay of the quasi-normal modes of the ringdown), respectively, and are therefore expected to produce better results for a matched-filter search for high-mass signals.

4. Results

4.1. Efficiency for detection

The main results of our search for numerical relativity signals injected in simulated LIGO noise employing a phenomenological template bank are presented in table 1. We show here a summary of the found triggers at different stages of the pipeline for several runs, with the starting frequency for the matched-filter integral being either 30 or 40 Hz and the integration stopping at three different frequencies—ISCO, light ring and LRD—displayed in ascending order. We have separated our results in two sections, according to performance in recovering the full set of 126 NINJA injections and the reduced set of 67 injections whose total mass falls below 160 $M_\odot$. This choice is motivated by the construction of the phenomenological bank discussed in section 3.

A time window of 120 ms has been used in order to cluster the triggers found by the pipeline in a single detector. Similarly the coincidence has been determined within a 80 ms injection window. Given these choices for the parameters used in clustering the triggers, we

Table 1. Results of the search for NINJA signals using the phenomenological template bank. There were 126 injections performed into the analysed data for H1, H2 and L1, 67 of which fell within the mass range of our phenomenological template bank ($M < 160\,M_\odot$). We explicitly show that a much better efficiency in trigger recovery is achieved when the cutoff frequency is pushed beyond the ISCO frequency, up to the light ring and Lorentzian ringdown frequencies. Likewise we observe improved efficiency in finding the signals that lie within the mass range of our template bank. In both cases the signal-based vetoes have little influence in the rejection of triggers, confirming their efficiency in separating inspiral-like signals from other kind of glitches.

Frequency cutoff	ISCO	LightRing	LRD	LRD
Filter start frequency	30 Hz	30 Hz	30 Hz	40 Hz
Complete set of 126 NINJA injections				
Found single (H1, H2, L1)	78, 54, 69	94, 66, 90	92, 61, 87	93, 60, 86
Found coincidence	59	78	81	80
Found second coincidence	59	78	80	79
Reduced set of 67 NINJA injections with $M < 160\,M_\odot$				
Found single (H1, H2, L1)	40, 17, 32	55, 41, 50	55, 41, 50	56, 40, 50
Found coincidence	30	47	48	47
Found second coincidence	30	47	48	47

report recovery of 80/126 triggers in double or triple coincidence for the full injection set and 48/67 triggers for the reduced set with $M < 160\,M_\odot$. These are triggers that survive the second coincidence stage (including the signal-based vetoes) for our best run, which corresponds to the matched-filter integral starting at 30 Hz and ending at the LRD frequency. The number of recovered triggers in the full mass range is compatible with the results quoted by other participants in the NINJA project employing searches with higher-order corrections PN templates extended up to larger frequencies, such as the effective ringdown (ERD) and weighted ringdown (WRD) ending frequencies (see [41] for definitions). The efficiency of the search improves, however, when we restrict ourselves to signals with masses overlapping those of our template bank. It is worthwhile noting that among the triggers recovered by the pipeline we find not only non-spinning simulations but also signals with non-precessing spins, such as the CCATIE and BAM_BBH waveforms (except in the case of equal $S/m^2 = 0.25$ spins aligned in the z-direction[2], which we discuss later). This supports existing evidence for the fact that non-spinning templates should be able to detect non-precessing spinning signals with moderate individual spins. The capability of non-spinning templates for recovering signals with precession and large spins could however be compromised, as we discuss below. Due to the low statistics of the present analysis, these statements should be taken with the appropriate reservations.

Figure 3 provides an overview of the found and missed injections corresponding to total mass below $160\,M_\odot$. The colour code encodes the modulus of the dimensionless total spin $\left|\vec{S}_1/m_1^2 + \vec{S}_2/m_2^2\right|$ of the black holes, and gives an indication of the injections that significantly deviate from the non-spinning case modelled by the phenomenological waveforms. We observe how signals located at distances above 350 Mpc are systematically lost, giving us an indication of the distance reach of the pipeline; nevertheless, several nearby injections are missed as well. In order to track down the missed injections in the mass region below $160\,M_\odot$, a compilation of their relevant physical parameters and associated information is given in table 2. For a description of the diverse NR simulations listed therein we refer the reader to

[4] Here S is the modulus of the angular momentum $\vec{S}$ (which in this particular BAM simulation is the same for both black holes).

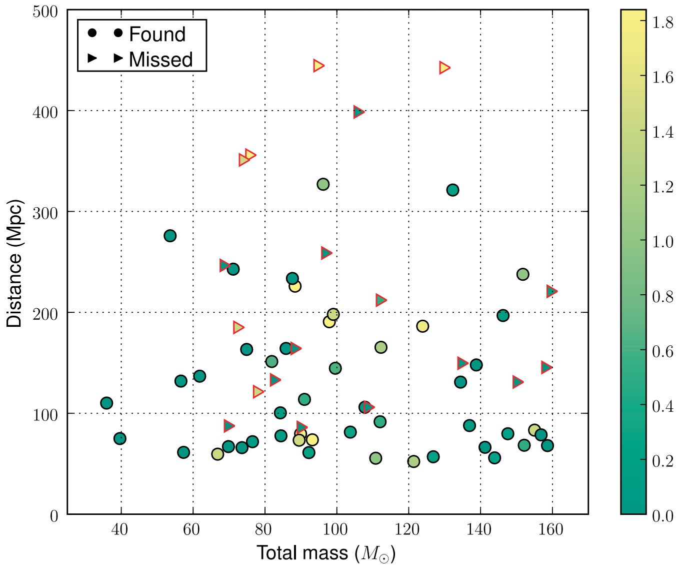

Figure 3. The figure shows found and missed injections in the mass region $32\,M_\odot \leqslant M \leqslant 160\,M_\odot$ as a function of their total mass and distance for our best search, starting at 30 Hz and stopping at the LRD frequency. The circles represent triggers that were recorded as either double or triple coincidences after the second stage (including the signal-based vetoes), whereas the triangles represent missed injections. The colour code displayed in the vertical scale represents the modulus of the dimensionless total spin $|\vec{S}_1/m_1^2 + \vec{S}_2/m_2^2|$ of the black holes. The red border of the triangles serves solely as visual aid to facilitate their quick identification as missed injections.

[41]. A similar analysis of the missed and found injections has been recently performed by the Birmingham group in [52], applying Bayesian inference on the NINJA data using a nested sampling algorithm. The work of Aylott *et al* explores how different waveform families affect the confidence of detection of NR waveforms. Their Bayes factor B is a metric for assessing the level of confidence that a signal has been detected, and their defined thresholds for $\log_{10} B$ allow for classification of the signals as found or missed. The IDs displayed in bold type in table 2 correspond to signals that are reported as missed by the Birmingham group in table 2 of [52]; 12 of our 19 missed injections are also lost by them, a correlation that seems worth following up. Future versions of the NINJA project will certainly benefit from combined searches and cross-checks of this kind between different DA methods.

Signals with large eccentricity, such as the Princeton $e \gtrsim 0.5$ `PU_T52W` run are invariably lost by our pipeline. Likewise, the phenomenological templates are not able to pick up signals with considerable spin, such as the equal-mass, spinning waveforms from `LazEv` with individual spins of equal value $S/m^2 = 0.92$ aligned along the z-axis and `BAM_FAU` with precessing spins $S/m^2 = 0.75$ outside the xy-plane and misaligned with respect to the z-direction. Our template bank was developed to search for signals in which spin is unimportant and no precession is present, so these results are understandable. Further work targeted to incorporating spins within the phenomenological model is desirable and will be undertaken in the future. The missed `GSFC` signals with mass ratio 1:3 and 1:4 correspond to runs with few orbits before merger and moreover they are injected at total masses bordering on the edge of our template bank, which could explain them being lost. More bewildering is however the fact that the pipeline misses a couple of long equal-mass non-spinning simulations injected at rather close distances, such as `CaltechCornell`, which is also missed by the search reported

Table 2. Overview of the 19 missed injections with total mass below 160 $M_\odot$ for the best run reported. The ID column stores an index that identifies each of the injections of the NINJA set. The convention for the naming of the NR simulations can be found in [41]. The last column displays the modulus of the sum of the black-holes individual spins. Among the missed signals we stress the presence of waveforms with eccentricity, large spins and precession and also those injected at distances further than 350 Mpc. Note that the boldfaced IDs correspond to signals also reported as missed in [52], where a Bayesian inference search on the NINJA data using a nested sampling algorithm is presented.

ID	NR simulation	Total mass ($M_\odot$)	Distance (Mpc)	Effective distance H (Mpc)	Effective distance L (Mpc)	η	Total spin $\lvert\sum \vec{S}_i/m_i^2\rvert$
136	`LazEv`	94.6	444.5	15 831.9	2941.3	0.25	1.84
141	`LazEv`	75.6	355.8	1047.2	746.6	0.25	1.84
142	`LazEv`	129.7	442.5	2221.8	1537.7	0.25	1.84
59	`CC`	69.7	87.5	469.2	1573.0	0.25	0
41	`BAM_HHB_spp25`	112.0	212.1	1150.8	802.2	0.25	0.5
47	`BAM_HHB_spp00`	150.0	131.0	648.5	908.0	0.25	0
27	`BAM_FAU`	77.8	121.3	764.1	741.1	0.25	1.43
29	`BAM_FAU`	72.3	185.1	1325.7	885.4	0.25	1.43
30	`BAM_FAU`	73.9	351.1	896.9	771.4	0.25	1.43
114	`PU_T52W`	82.6	133.1	364.0	320.2	0.25	0
116	`PU_T52W`	88.2	164.2	654.7	533.7	0.25	0
118	`PU_T52W`	90.0	86.0	1055.4	452.3	0.25	0
120	`PU_T52W`	108.6	106.0	202.0	205.9	0.25	0
125	`PU_T52W`	96.8	258.8	463.8	464.7	0.25	0
126	`PU_T52W`	105.8	398.5	1175.2	1797.1	0.25	0
64	`GSFC_X4`	134.7	149.6	1320.4	856.0	0.16	0
68	`GSFC_X3`	160.0	220.8	819.3	1123.2	0.1875	0.222
76	`GSFC_X4`	158.0	145.4	722.2	558.5	0.16	0
95	`Lean_c138`	68.6	246.5	333.9	407.7	0.16	0
			Total number of missed injections: 19				

in [52], and `BAM_HHB_spp00`. A look at the columns of table 2 that list the *effective distance* in H and L (the distance to an equivalent source with optimal location and orientation) indicates that it might be the poor orientation of these injections that prevents the pipeline from finding them. Aside from these individual cases, which would need a careful follow-up that is below the scope of this paper, we can justify the rest of missed injections as those either placed at large distances, presenting large spin values and/or precession and containing few orbits before merger.

Among the obvious improvements that a search with phenomenological templates could benefit from we can mention the following. First, and once the technical issue with the generation of high-mass templates is resolved, the search would clearly improve with the use of a template bank that fully covers the parameter space of the signals searched for. Additionally, the inclusion of the fourth interferometer V1 in our pipeline shall provide a larger number of recovered triggers, in the manner reported by the search using EOBNR templates that is described in section 4.1.3 of [41]. Both improvements will be most likely incorporated to searches with the phenomenological template bank in future realizations of the NINJA project.

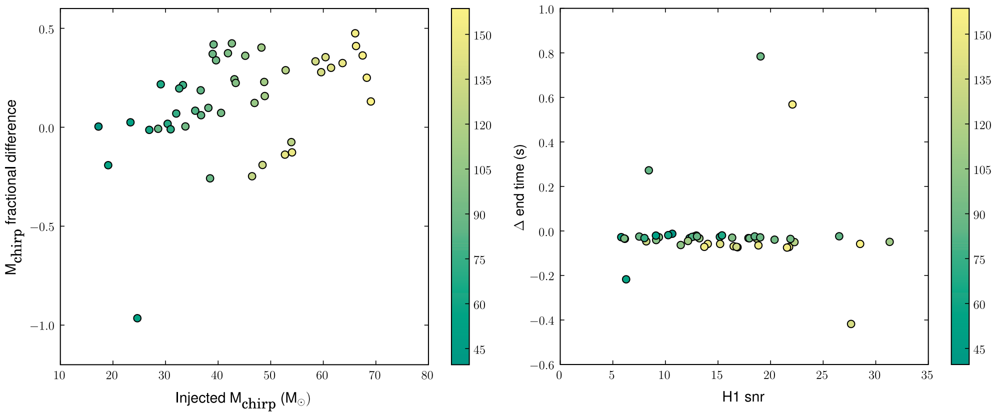

Figure 4. Figures showing the accuracy with which the chirp mass (left panel) and end time (right panel) of the reduced set of NINJA injections with total mass below 160 $M_\odot$ are recovered using the phenomenological template bank. In both plots, the colour scale is given by the total mass of the system. The chirp mass, a common quantity in data analysis which is defined as $\mathcal{M} = (m_1 m_2)^{3/5}(M)^{-1/5}$, is typically recovered within a 20%–40% accuracy, depending on the chirp mass and total mass of the system. On the right panel, we observe a few low-mass outliers that would need a more careful follow-up. Nevertheless, the results for parameter estimation with our IMR bank constitute a significant improvement over current LIGO/Virgo searches with standard PN templates.

4.2. Accuracy for parameter estimation

The number of found versus missed triggers is not the only relevant metric for assessing the performance of the standard GW searches. If astrophysically relevant statements are to be made from GW observations, the ability of accurately estimate the physical parameters of the measured signals is crucial. The inspiral pipeline returns estimated values for the individual and total masses of the detected system, effective distance, coalescence time and event duration, among others. Figure 4 shows two parameter estimation plots for the phenomenological search on the NINJA injections. The left panel displays the fractional difference for recovery of the chirp mass of the system, defined as $\mathcal{M} = (m_1 m_2)^{3/5}(M)^{-1/5}$. The vertical colour bar encodes the total mass in solar masses. We report substantial improvement in parameter estimation with respect to LIGO/Virgo standard searches that make use of PN templates, which we can see in figure 8 of the NINJA paper [41]. While standard PN searches recover most of the injections with a fractional difference in chirp mass of 0.5 or above, the left panel of figure 4 shows an overall better accuracy, with the exception of one outlier. Using the phenomenological template bank, the chirp mass is recovered within a 20% accuracy for values of $\mathcal{M}$ below 40 $M_\odot$ and ∼40% for signals with larger chirp mass. In any case, it should not be forgotten that the PN searches reported in [41] make use of banks with masses up to 90 $M_\odot$ only. The outlier that can be spotted at $\mathcal{M} \sim 30\, M_\odot$ corresponds to a `CaltechCornell` waveform injected at 132 Mpc with total mass 56.6 $M_\odot$. For this particular injection the accuracy in parameter recovery is rather poor, and further work to understand this behaviour will be undertaken in the future.

The panel in the right shows the accuracy in end time recovery of the found signals, with the colour code again displaying the total mass of the system. The injection time of the numerical waveforms corresponds to the maximum of their amplitude, which happens roughly at the merger of the two black holes. Current PN templates stop before that point while IMR templates extend beyond the merger into the ringdown. The sign convention for $\Delta t_{\rm end}$ corresponds to the injected minus the recovered parameters, so that a trigger that presents a positive value $\Delta t_{\rm end} > 0$ indicates that the signal was really injected at a *later* time than the value recorded by our pipeline. Most of the signals displayed in the left panel of figure 4 are recovered at a time within a few hundredths of second from the injected end time value, with the outliers corresponding partially to signals with larger total mass. These results are consistent with the other IMR search reported in the NINJA paper. Again we expect that the use of a template bank overlapping the mass region of the injections would lead to a reduction of the outliers, but certain improvement with respect to the left panel in figure 8 of [41] can still be acknowledged.

Even though the number of total recovered triggers for the phenomenological search on the NINJA data is similar to the results quoted by the standard PN searches, there is a reasonable indication that the use of a full IMR template bank helps the estimation of the physical signal parameters. In view of these and other coincident results quoted in [41, 52, 53], we conclude that searches that attempt to recover and estimate the physical parameters of BBH signals in the mass range 10^2–$10^3\,M_\odot$ would profit from using an IMR template bank that fully models the inspiral, merger and ringdown of the binary system. This is of crucial important for future LIGO/Virgo searches that aim at targeting coalescences of compact objects in the above-mentioned range, for which a full template bank adapted to arbitrarily high masses (and ideally also to non-zero spin values) needs to be developed. Attempts in this direction are already underway within the LIGO/Virgo Collaboration.

5. Conclusion

We have presented the results from the first search using the standard inspiral pipeline modified to match-filter against the phenomenological template bank introduced by Ajith *et al*, an inspiral-merger-ringdown template that models the full coalescence of non-spinning black-hole binaries of small mass ratios. This procedure has been directly applied to the search for numerically simulated signals injected into simulated LIGO noise within the frame of the NINJA Collaboration. We have tried several values for the cutoff frequency in the match-filter integral and found results that corroborate the need for pushing the integration to higher values than the ISCO if one wants to pick up signals that contain information about the merger and ringdown stages of the BBH coalescence process, which is very relevant for LIGO/Virgo high-mass searches. The total number of NINJA signals that we are able to recover using the phenomenological template bank is comparable to the results reported by other groups that participated in the NINJA project searching with PN templates extended to higher frequencies. Nevertheless, improved accuracy in parameter recovery is obtained with our phenomenological template bank. Moreover, it is expected that, had we constructed a bank covering the exact parameter space of the NINJA injections and included the fourth V1 detector in our analysis, the number of recovered triggers would have significantly increased. This information will be used as starting point in future applications of the phenomenological waveforms to the search for inspiral signals.

There are however a number of signals that are not found by our pipeline and that we have identified as injections falling outside the parameter space of our template bank, injections placed at distant locations above 350 Mpc, poorly oriented injections and injections corresponding to evolutions of black holes with significant eccentricity, spins and precession, plus a few outliers that undoubtedly need a more careful and dedicated study. More precise statements on found and missed signals would nevertheless require larger statistics in our data.

There are several obvious improvements in the construction of the phenomenological waveform model that can be made. The phenomenological waveforms have so far been constructed only for the dominant mode of the comparable mass non-spinning case and it is not surprising that, for example, some waveforms with precession or eccentricity are not recovered. Searches for spinning objects are of the greatest astrophysical importance, and phenomenological or other types of theoretical models for these kind of systems are much needed. The phenomenological ansatz used to fit the merger portion (especially the power law for the amplitude) needs to be extended to higher mass ratios and spins. The error bars on the phenomenological parameters need to be better quantified, and the matching to post-Newtonian theory done as early in the inspiral phase as possible, and higher modes included. Notwithstanding, our results show a clear improvement in parameter estimation when the full inspiral-merger-ringdown waveform is used as template. This result is confirmed by other reports within the frame of the NINJA Collaboration. Future research on phenomenological models comprises development of adequate phenomenological waveforms targeted at getting better detection and parameter estimation of signals from black-hole binaries in the current LIGO/Virgo data-analysis pipelines. Work on these improvements is in progress, and will be applied in future NINJA projects.

Acknowledgments

The authors thank S Fairhurst, B Farr, E Ochsner, B Satyaprakash, M Hannam, S Husa and L Pekowski for useful comments and helpful suggestions while this analysis was being carried out. We acknowledge hospitality from the Kavli Institute for Theoretical Physics (KITP) Santa Barbara during the workshop ‘Interplay between Numerical Relativity and Data Analysis’, where the NINJA project was initiated; the Kavli Institute is supported by NSF grant PHY 05-51164. This work was supported by the Max Planck Society, by DFG grant SFB/TR 7, by the German Aerospace Center (DLR) and by the National Science Foundation under grant NSF-0838740. LS is partially supported by DAAD grant A/06/12630. This paper has been assigned LIGO document number P080125-01-Z.

References

[1] Abbott B *et al* (LIGO Scientific Collaboration) 2007 arXiv:0711.3041
[2] Acernese F *et al* 2006 *Class. Quantum Grav.* **23** S635–S642
[3] Hild S (for the LIGO Scientific Collaboration) 2006 *Class. Quantum Grav.* **23** S643–S651
[4] Danzmann K *et al* 1998 *Max-Planck-Inisitut für Quantenoptik, Report MPQ* vol 233 184–209
[5] Danzmann K and Rüdiger A 2003 *Class. Quantum Grav.* **20** S1–S9
[6] Blanchet L 2006 *Living Rev. Rel.* **9** (http://www.livingreviews.org/lrr-2006-4)
[7] Pretorius F 2005 *Phys. Rev. Lett.* **95** 121101 (arXiv:gr-qc/0507014)
[8] Campanelli M, Lousto C O, Marronetti P and Zlochower Y 2006 *Phys. Rev. Lett.* **96** 111101 (arXiv: gr-qc/0511048)
[9] Baker J G, Centrella J, Choi D I, Koppitz M and van Meter J 2006 *Phys. Rev. Lett.* **96** 111102 (arXiv: gr-qc/0511103)
[10] Abbott B *et al* (LIGO Scientific Collaboration) 2008 *Phys. Rev.* D **77** 062002 (arXiv:0704.3368)
[11] Abbott B *et al* (LIGO Scientific Collaboration) 2009 arXiv:0901.0302
[12] LSC Algorithm Library (LAL) http://www.lsc-group.phys.uwm.edu/lal
[13] Buonanno A *et al* 2007 *Phys. Rev.* D **76** 104049 (arXiv:0706.3732)
[14] Ajith P *et al* 2007 *Class. Quantum Grav.* **24** S689–S699 (arXiv:0704.3764)
[15] Ajith P *et al* 2008 *Phys. Rev.* D **77** 104017 (arXiv:0710.2335)
[16] Ajith P 2008 *Class. Quantum Grav.* **25** 114033 (arXiv:0712.0343)
[17] Numerical injection analysis (NINJA) project https://www.gravity.phy.syr.edu/dokuwiki/doku.php?id=ninja:ho me
[18] Brügmann B *et al* 2008 *Phys. Rev.* D **77** 024027 (arXiv:gr-qc/0610128)

[19] Husa S, González J A, Hannam M, Brügmann B and Sperhake U 2008 *Class. Quantum Grav.* **25** 105006 (arXiv:0706.0740)

[20] Alcubierre M *et al* 2000 *Phys. Rev.* D **62** 044034 (arXiv:gr-qc/0003071)

[21] Alcubierre M *et al* 2003 *Phys. Rev.* D **67** 084023 (arXiv:gr-qc/0206072)

[22] Koppitz M *et al* 2007 *Phys. Rev. Lett.* **99** 041102 (arXiv:gr-qc/0701163)

[23] Pollney D *et al* 2007 *Phys. Rev.* D **76** 124002 (arXiv:0707.2559)

[24] Imbiriba B, Baker J, Choi D I, Centrella J, Fiske D R, Brown J D, van Meter J R and Olson K 2004 arXiv:gr-qc/0403048

[25] van Meter J R, Baker J G, Koppitz M and Choi D I 2006 *Phys. Rev.* D **73** 124011 (arXiv:gr-qc/0605030)

[26] Zlochower Y, Baker J G, Campanelli M and Lousto C O 2005 *Phys. Rev.* D **72** 024021 (arXiv:gr-qc/0505055)

[27] Sperhake U 2007 *Phys. Rev.* D **76** 104015 (arXiv:gr-qc/0606079)

[28] Hinder I, Vaishnav B, Herrmann F, Shoemaker D and Laguna P 2008 *Phys. Rev.* D **77** 081502 (arXiv:0710.5167)

[29] Pretorius F 2005 *Class. Quantum Grav.* **22** 425–52 (arXiv:gr-qc/0407110)

[30] Scheel M A *et al* 2006 *Phys. Rev.* D **74** 104006 (arXiv:gr-qc/0607056)

[31] Etienne Z B, Faber J A, Liu Y T, Shapiro S L and Baumgarte T W 2007 *Phys. Rev.* D **76** 101503 (arXiv:0707.2083)

[32] Hannam M, Husa S, Sperhake U, Brügmann B and González J A 2008 *Phys. Rev.* D **77** 044020 (arXiv:0706.1305)

[33] Hannam M, Husa S, Brügmann B and Gopakumar A 2008 *Phys. Rev.* D **78** 104007 (arXiv:0712.3787)

[34] Tichy W and Marronetti P 2008 *Phys. Rev.* D **78** 081501 (arXiv:0807.2985)

[35] Rezzolla L *et al* 2008 *Astrophys.* J **679** 1422–6 (arXiv:0708.3999)

[36] Vaishnav B, Hinder I, Herrmann F and Shoemaker D 2007 *Phys. Rev.* D **76** 084020 (arXiv:0705.3829)

[37] Buonanno A, Cook G B and Pretorius F 2007 *Phys. Rev.* D **75** 124018 (arXiv:gr-qc/0610122)

[38] Pretorius F and Khurana D 2007 *Class. Quantum Grav.* **24** S83–S108 (arXiv:gr-qc/0702084)

[39] Boyle M *et al* 2007 *Phys. Rev.* D **76** 124038 (arXiv:0710.0158)

[40] Scheel M A *et al* 2008 arXiv:0810.1767

[41] Aylott B *et al* 2009 arXiv:0901.4399

[42] Allen B, Anderson W G, Brady P R, Brown D A and Creighton J D E 2005 arXiv:gr-qc/0509116

[43] Owen B J 1996 *Phys. Rev.* D **53** 6749–61 (arXiv:gr-qc/9511032)

[44] Babak S, Balasubramanian R, Churches D, Cokelaer T and Sathyaprakash B 2006 *Class. Quantum Grav.* **23** 5477–504 (arXiv:gr-qc/0604037)

[45] Cokelaer T 2007 *Phys. Rev.* D **76** 102004 (arXiv:0706.4437)

[46] Robinson C A K, Sathyaprakash B S and Sengupta A S 2008 *Phys. Rev.* D **78** 062002 (arXiv:0804.4816)

[47] Allen B 2005 *Phys. Rev.* D **71** 062001 (arXiv:gr-qc/0405045)

[48] Rodríguez A 2007 Reducing false alarms in searches for gravitational waves from coalescing binary systems *Master's Thesis* Louisiana State University (http://www.ligo.caltech.edu/docs/P/P070056-00.pdf)

[49] Brügmann B, González J A, Hannam M, Husa S, Sperhake U and Tichy W 2008 *Phys. Rev.* D **77** 024027 (arXiv:gr-qc/0610128)

[50] Damour T, Nagar A, Hannam M, Husa S and Brügmann B 2008 *Phys. Rev.* D **78** 044039 (arXiv:0803.3162)

[51] Damour T, Iyer B R and Sathyaprakash B S 2000 *Phys. Rev.* D **62** 084036 (arXiv:gr-qc/0001023)

[52] Aylott B, Veitch J and Vecchio A 2009 in preparation

[53] Farr B, Fairhurst S and Sathyaprakash B S 2009 arXiv:0902.0307

[54] Berti E, Cardoso V and Will C M 2006 *Phys. Rev.* D **73** 064030